

Effect of hydrothermal curing on early hydration of G-Oil well cement

Martin Palou · Vladimír Živica · Tomáš Ifka ·
Martin Boháč · Martin Zmrzlý

Received: 13 August 2013 / Accepted: 4 November 2013 / Published online: 24 November 2013
© Akadémiai Kiadó, Budapest, Hungary 2013

Abstract G-Oil well cement has been cured under standard and hydrothermal conditions with different steam pressures and temperatures. Compressive strength, pore structure parameters, microstructure, and hydrated products were evaluated after 7 days curing by using SEM, MIP, and simultaneous TGA/DSC. Obtained results showed that 7 days aged sample cured under standard conditions has the highest compressive strength with compact pore structure and hydrated products similar to those found after hydration of Ordinary Portland cement. With increasing temperature and pressure from standard conditions (25 °C, 10125 Pa) to hydrothermal ones (150 °C and 0.3 MPa, 200 °C and 1.2 MPa), compressive strength has drastically decreased from 77.5 ± 2.0 to 20.5 ± 1.0 MPa due to the transformation of original hydrated products (C–S–H) to crystallized α -C₂SH and C₆S₂H₃. The crystallization has led, under hydrothermal curing, to the increase of permeability and pore structure depletion. The final compressive strength after curing for 7 days at 150 °C (51.8 ± 2.0 MPa) and 200 °C (20.5 ± 1.0 MPa), which significantly exceeds the recommended values of 3.45 MPa according to API to hold many casings of oil wells is questionable for application in geothermal ones.

Keywords Hydrothermal curing · Thermal decomposition · Microstructure · Pore structure · Compressive strength

Introduction

The hydration reaction of Ordinary Portland cement (OPC) is a complex chemical and physical processes that take place after contact of the anhydrous solid with water resulting in the formation of new products responsible for consolidation, strength development, and durability of constructions. The hydration runs via chemical reaction between different minerals of cement (C₃S, C₂S, C₃A, and C₄AF) and water to form gelatinous or semi-crystalline calcium silicate hydrate, denoted C–S–H; calcium sulfoaluminate hydrate (ettringite or monosulfate), and calcium hydroxide (CH) giving appropriate strength and durability to hardened cement paste, mortars, or concrete. As cement is used under different climatic conditions, the temperature becomes a pertinent key factor that influences the kinetics and mechanism of hydration, and the nature of hydrated products. Many studies have investigated the temperature dependence of the rate of hydration, and found that it can be described by an Arrhenius equation [1–3]. As the nature of hydrated changes with temperature, authors [4, 5] have investigated hydration of OPC under different saturated steam pressure at temperature range 120–350 °C. The defined system hydrated to form different calcium silicate hydrates. Up to 110 °C tobermorite (Ca₅Si₆O₁₆(OH)_{2.4}(H₂O)) is formed and between 120 and 350 °C α -C₂SH and xonotlite (Ca₆Si₆O₁₇(OH)₂) associated with volume reduction appear as major products with an increase in porosity. Consequently, concrete under high temperature undergoes strength retrogression due to enumerated transformations and reactions, causing progressive breakdown of cement gel structure and loss in its

The standard nomenclature of cement chemistry is used: C = CaO, A = Al₂O₃, F = Fe₂O₃, S = SiO₂, H = H₂O.

M. Palou (✉) · V. Živica · T. Ifka
Institute of Construction and Architecture, Slovak Academy of
Sciences, Dúbravská cesta, 9 845 03 Bratislava 45, Slovak
Republic
e-mail: martin.palou@stuba.sk; martin.palou@savba.sk

M. Palou · M. Boháč · M. Zmrzlý
Faculty of Chemistry, Brno University of Technology,
Purkyňova 464/118, 612 00 Brno, Czech Republic

load-bearing capacity, reduced durability, and increased tendency of drying shrinkage, structural cracking, and associated aggregate color changes [6].

Next to temperature, humidity is a determinant factor for the hydration of cement paste. It can prevent the shrinkage of concrete during the early period of applications. The coupled effect of elevated temperatures and steam pressure in environments denoted as hydrothermal ones, are a common characteristic of geothermal, oil, and gas wells [7–12]. In these environments, temperatures and pressures are so high (up to 200 °C and 150 MPa in deep wells) that they challenge the capabilities of construction materials used in the wells. For this purpose, cement slurry is placed in the annular space between the well steel casing and the geological formations surrounding the well bore in order to provide zonal isolation, preventing thus corrosion of steel casing and ensuring pipe strength improvement in oil, gas, and water wells. Cement forms an extremely strong, nearly impermeable seal from a thin slurry. Incomplete zonal isolation and/or a weak hydraulic seal between the casing and the cement and between the cement and the formations may cause oil spills and the well may never run at its full producing potential [13]. Thus, oil and gas well cementing operations face additional challenges in contrast to common cementing work above ground. In addition to the high pressure and temperature, oil well cements must be able to contend with weak or porous formations, corrosive fluids, etc. A successful oil well cementing must have low permeability and adequate durability to ensure the long-term isolation of the producing formation. The type of cement depends on a type of high temperature, pressure, depth, and chemical composition of environments. For cementing these wells as protective layer of dwell during the exploitation of natural gas and petroleum [14], the API (American Petroleum Institute) specifications for materials and testing for well cements (API Specification 10A, 2002) has established nine special classes of cements (Class A–Class J). They are arranged according to the depths, to which they are placed, and the pressures and temperatures to which they are exposed [14]. Oil well cements are usually made from Portland cement clinker or from blended hydraulic cements.

The investigation of hydrothermal curing conditions on the behaviors of oil wells cement is an important task required not only for the oil industries but also for those researchers involved in development of new cementing materials for more severe hydrothermal conditions of application. Furthermore, there has been comparatively less work done on the pressure effect on hydration of cement.

The literature contains many references pertaining to calcium silicate hydrates in wells at temperatures up to 150 °C, but little has been published concerning higher temperatures associated with steam pressure. The present study attempts to develop a better understanding of the

coupled effects of temperature and pressure on early hydration of G-Oil well cement. The G-Oil cement paste was cured under standard and hydrothermal conditions of 0.3 MPa (150 °C) and 1.2 MPa (200 °C).

Experimental

The kind of hydration products formed under hydrothermal conditions and their stability was investigated by simultaneous thermal analysis (DTA and TG) Mettler-Toledo TGA/DSC STRA system (Mettler-Toledo, Switzerland), where sample was placed in an open vessel under air atmosphere, and measured at a heating rate of 10 °C min⁻¹ up to 1,000 °C.

Autoclave and hydrothermal conditions used the pressure of 0.3 MPa (150 °C) and 1.2 MPa (200 °C), and the duration of autoclaving was 7 days. At chosen time of autoclaving, the hot prisms was taken off and inserted in hot water. Cooling of water was accelerated gradually by adding of cold water as the handling temperature of ~40 °C was achieved.

Mercury intrusion porosimeter Quantachrome Poremaster 60GT (Quantachrome UK Limited) was used for the determination of pore structure characteristics (total porosity, distribution of pore sizes, and permeability). Two or three pieces of the dried sample with diameter less than 10 mm and total mass max. 2 g were used for the tests. The maximum applied pressure of mercury was 414 MPa, equivalent to a Washburn pore radius of 1.8 nm.

Scanning electron microscope, JEOL JSM-7600F equipped with EDX was used for microstructure observations.

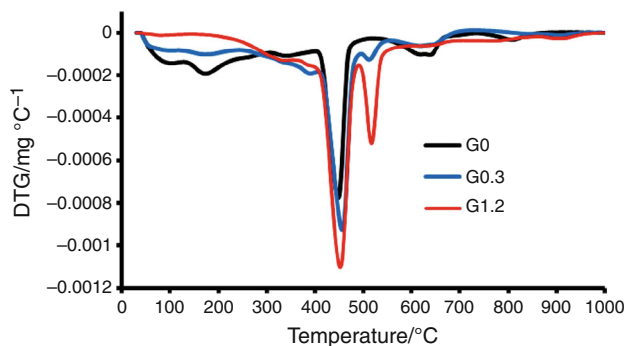
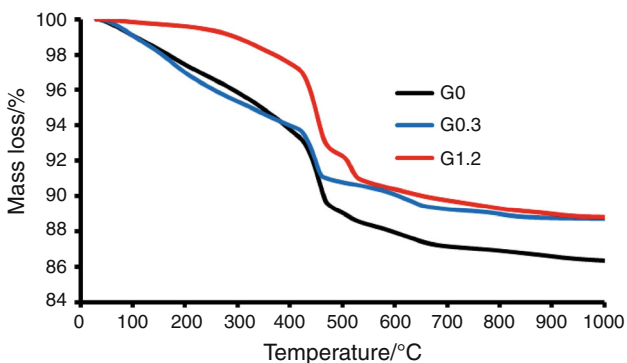
Oil well Portland cement without mineral components denoted as Class G HSR was from Holcim OJSC “Volskement”, Saratov region, Russia. The chemical composition of cement (%) and mineralogical composition of clinker (%) given by the producer are reported in Table 1.

Mixing procedure and test specimens

Appropriate pastes were prepared by mixing oil well cement with adequate quantity of water as determined by workability procedure (water to cement ratio of 0.35). Six prisms with the dimensions of 160 mm × 40 mm × 40 mm were prepared from paste to be cured under various conditions during 7 days. *G0* denotes samples cured under standard condition of 20 °C and 100 % rel. humidity, *G0.3* represents those cured under hydrothermal condition of 0.3 MPa (150 °C), and *G1.2* those cured under thermal condition of 1.2 MPa (200 °C). The specimens were exposed to steam curing condition at 100 °C for 30 min and after this pre-

Table 1 Oxide and mineralogical composition of oil well cement G

| Cement oxide | | Clinker minerals | | |
|-------------------------|---------------|---|---|---------------|
| Oxide | Composition/% | Designation | Formula | Composition/% |
| CaO | 64.0 | Alite | $3\text{CaO}\cdot\text{SiO}_2$ | 65.0 |
| SiO_2 | 21.0 | Belite | $2\text{CaO}\cdot\text{SiO}_2$ | 12.0 |
| Al_2O_3 | 4.5 | Aluminates | $3\text{CaO}\cdot\text{Al}_2\text{O}_3$ | 2.5 |
| Fe_2O_3 | 5.5 | Aluminate–ferrites | $4\text{CaO}\cdot\text{Al}_2\text{O}_3\cdot\text{Fe}_2\text{O}_3$ | 17.5 |
| MgO | 1.5 | Sum $3\text{CaO}\cdot\text{Al}_2\text{O}_3 + 4\text{CaO}\cdot\text{Al}_2\text{O}_3\cdot\text{Fe}_2\text{O}_3$ | | 22.5 |
| SO_3 | 2.5 | | | |

**Fig. 1** DTG curves of G-Oil well cement cured under standard condition and hydrothermal curing (G0, G0.3, and G1.2)**Fig. 2** TG curves of G-Oil well cement cured under standard condition and hydrothermal curing (G0, G0.3, and G1.2)

curing procedure still hot hardened specimens were quickly demolded and inserted into the autoclave. In each curing time, three samples were implemented and average values of the compressive strength of samples were calculated and recorded as the total compressive strength in the corresponding time.

Results and discussion

The DTG and TG characteristics of samples *G0*, *G0.3*, and *G1.2* are depicted in Figs. 1 and 2. While the TG

measurements characterize progressive mass changes of the sample as it is being heated at controlled temperature rate, DTG curves express the rate of mass changes within a specific temperature range. TG and DTG serve to identify quantitatively and qualitatively the hydrated products formed during the hydrothermal curing.

Sample *G0* was cured under standard condition of 20 °C in environment with 100 % relative humidity. DTG curve (Fig. 1) of standardly cured oil well cement slurry shows that its hydration process is similar to that of Portland cement. The presence of C–S–H gel and ettringite in the hardened paste is indicated by the dehydration effects under 200 °C with peaks at 100 and 150 °C respectively. This result is also corroborated by mass loss curves obtained from TG curves showing substantial water losses in the range 100–200 °C (Fig. 2). The main endothermic peak is observed on DTG curve in the range of 400–500 °C with maximum at 450 °C. This peak results from the thermal degradation of $\text{Ca}(\text{OH})_2$ present in cured sample. Furthermore, it is evident that a part of hydrated product was carbonated, as it is demonstrated by two peaks between 600–700 and 800–900 °C. The total mass loss (Fig. 2) is 13.66 %, of which 30.16 % represents the part of water chemically bond in C–S–H and ettringite, 50 % in CH, and the rest results from the thermal decomposition of carbonated products, about 19.80 %.

Sample *G0.3* is oil well cement cured in hydrothermal condition with 0.3 MPa (150 °C) during 7 days. If the main product of hydration remains calcium hydroxide, it is clear that the effect of hydrothermal curing has led to the formation of new product with endothermic peak located at 520 °C and to slight increase of calcium silicate hydrates. Carbonation is less pronounced due to the isolated conduction in autoclave (Fig. 2). The nature of these products is subject of many controversial studies. It was documented by Ramachandran et al. [15] that $\alpha\text{-C}_2\text{SH}$ crystalline with high permeability is a product of thermal transformation of C–S–H under higher temperature and pressure conditions. In a modeled study of reaction between $\text{Ca}(\text{OH})_2$ and SiO_2 under hydrothermal curing conditions, Alunno et al. [16]

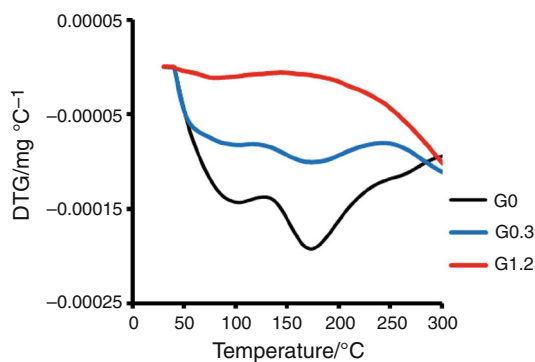


Fig. 3 DTG curve (50–300 °C) of G-Oil well cement cured under standard condition and hydrothermal curing (G0, G0.3, and G1.2)

has found that at high steam pressure the products obtained by hydration of C_3S are α - C_2SH , $C_6S_2H_3$ and $Ca(OH)_2$ after 5 h, but α - C_2SH decreases by increasing curing time. At 0.8–1.6 MPa the hydration products are α - C_2SH after 8 h and $C_6S_2H_3$ (jaffeite, similar properties as α - C_2SH) with trace of α - C_2SH after about 4 days. Midgley and Chopra [17] have found that a paste of C_3S hydrated for 7 days at 180 °C contained only $C_3S_2H_3$. From these findings, it is clear that the nature of hydrated products depends not only on hydrothermal curing conditions, but also on curing period. Differently from what has been reported by ones or another authors, one can postulate that in G-Oil well cement paste cured for 7 days at 150 and 200 °C the formation of $C_6S_2H_3$ has been occurred. It was reported by Collepari and Marches [18] that $C_6S_2H_3$ decomposes between 500 and 550 °C with peak at 530 °C. It cannot be excluded, however, that α - C_2SH has been prior formed and then transformed into $C_6S_2H_3$ under the effect of 7 days hydrothermal curing.

The total mass loss (Fig. 2) is 11.19 %, of which 41.46 % represents the part of water chemically bond in C–S–H and ettringite, 40.93 % in CH and α - C_2SH , and 4 % in $C_6S_2H_3$, and the rest results from the thermal decomposition of carbonated products, about 13.42 %. Carbonation is less pronounced under isolated autoclave curing conditions.

Sample G1.2 is cured under hydrothermal condition with 1.2 MPa (200 °C). The conditions are more severe. Figure 3 shows that the main change in the constitution of G-Oil cement paste occurs during autoclaving at 200 °C for 7 days. As a result of hydrothermal curing effect, calcium silicate hydrate (C–S–H) was almost disappeared, as it can be seen by the absence of endothermic peak (Fig. 1) in interval 100 and 130 °C at DTG curve and negligible mass loss at TG curve (Fig. 2). The hydration is more pronounced by an increase of CH.

The total mass loss (Fig. 2) is 11.19 %, of which 4.55 % can be attributed to the part of water chemically bond in

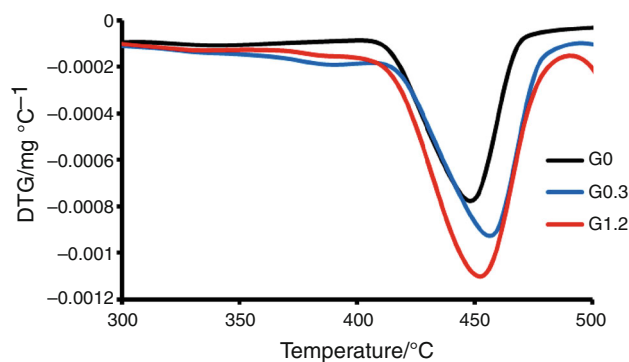


Fig. 4 DTG curve (300–500 °C) of G-Oil well cement cured under standard condition and hydrothermal curing (G0, G0.3, and G1.2)

C–S–H and ettringite, 64.52 % in CH and α - C_2SH , 16.90 % in $C_6S_2H_3$, and the rest 14 % results from the thermal decomposition of carbonated products.

As it was reported [7], when the well temperature exceeds 110 °C, the new abundant phase formed in the sample hydration of an oil well cement is α -dicalcium silicate hydrate α - C_2SH ($Ca_2SiO_3(OH)_2$), which forms bulk materials that are too weak and permeable to seal the well. According to authors [2, 8] α -CSH decomposes at 480 °C, but due to the overlapping of the thermal decomposition effect of CH at maximum 450 °C, the direct identification cannot be possible. The endothermic peak found at 518 °C is attributed to the thermal decomposition of $C_6S_2H_3$ (jaffeite) with negative effect on the performance of G-Oil well cement (Fig. 1).

Effect of hydrothermal curing on G-Oil well cement within different temperature intervals

50–300 °C: C–S–H products

Temperature range between 50 and 300 °C is characteristic for thermal decomposition of C–S–H and ettringite. It is evident that G0 cured under normal conditions presents two endothermic peaks at around 100 °C (C–S–H) and between 150 and 200 °C (ettringite). With increasing curing hydrothermal temperature (pressure), intensity of peaks characterizing the presence of two evoked hydrated products diminishes (150 °C/0.3 MPa) till they disappear under harsh hydrothermal conditions (200 °C/1.2 MPa). Quantitatively and qualitatively, the lessening of these peaks (Fig. 3) is due to the effect of hydrothermal temperature over the time on the C–S–H and ettringite leading to their degradation into $C_6S_2H_3$ (jaffeite) via α - C_2SH ($Ca_2SiO_3(OH)_2$) and monosulfate respectively. Then, $C_6S_2H_3$ (jaffeite) is later decomposed at 518 °C (Fig. 1).

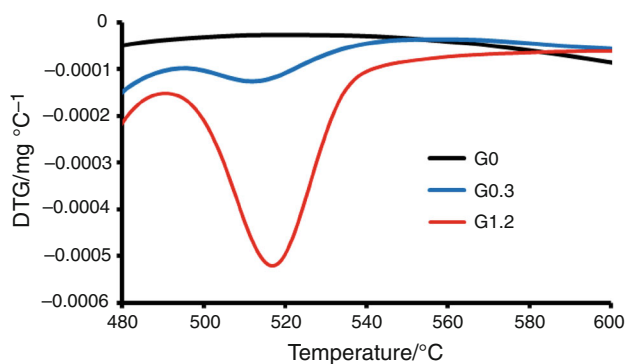
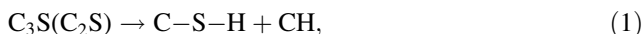


Fig. 5 DTG curve (480–600 °C) of G-Oil well cement cured under standard condition and hydrothermal curing (G0, G0.3, and G1.2)

300–500 °C: calcium hydroxide CH

At standard condition, tricalcium silicate (C_3S) and dicalcium silicate (C_2S), which comprise about 75 % of the dry Portland cement composition undergo a hydration reaction, which can be expressed by a general equation:



where C-S-H denotes gel or semi-crystalline calcium silicate hydrate with different C/S ratios and CH is calcium hydroxide [19, 20]. The calcium silicate hydrate (CSH) gel produced at low temperatures will convert to one or more crystalline phases upon curing at higher temperatures.

The presence of calcium hydroxide is characterized by endotherm in the vicinity of 450 °C. The endothermic peak intensity is proportional to the increasing curing temperatures. Indeed, a clear correlation between temperature range 0–200 and 300–500 °C can be established. Temperature accelerated hydration of C_3S and C_2S to CSH and CH. CSH is completely or partially transformed into $C_3S_2H_3$, but CH under isolated autoclaved conditions is not less carbonated (Fig. 4).

480–540 °C: $C_6S_2H_3$ (jaffeite)

The most indicative effect of hydrothermal curing effect is reported in Fig. 5 by the presence of endotherms located between 500 and 540 °C. As it was earlier reported, the endotherm found at this temperature range characterizes $C_6S_2H_3$ (jaffeite) presence. The intensity of this endotherm is more pronounced with G1.2, while no peak is found in G0 curve. $C_6S_2H_3$ (jaffeite) results from the hydrothermal transformation of C-S-H trough via α - C_2SH ($Ca_2SiO_3(OH)_2$).

580–900 °C: weak calcium carbonate—calcite

In this temperature, two endotherms are observed: one between 620 and 660 °C highlighted in sample cured under

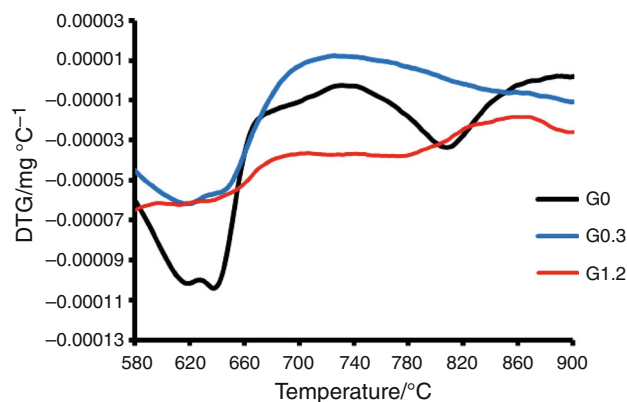


Fig. 6 DTG curve (580–900 °C) of G-Oil well cement cured under standard condition and hydrothermal curing (G0, G0.3, and G1.2)

standard condition and the second one between 740 and 960 °C. The peak positions are slightly moved toward lower temperatures with hydrothermal temperatures. While the first endotherm may characterize calcium carbonate like waterite, the second one represents the thermal decomposition of calcite. Quantitatively, carbonation is not pronounced as in standard conditions, since curing runs in isolated autoclave system (see Fig. 6).

The microstructures of samples cured under different conditions are shown in Fig. 7. Under standard conditions, unhydrated original cement mineral is still found after 7 days of curing. SEM investigation shows a dense paste structure. The unhydrated minerals are surrounded by a thin layer of binding mass C-S-H hydrates and $Ca(OH)_2$ with micropores.

Microstructure of sample cured in autoclave at hydrothermal pressure of 0.3 MPa shows a matrix with still unreacted mineral phases, but at lower extent. The hydration products appear as relatively dense in a homogenous matrix.

Sample cured under hydrothermal pressure of 1.2 MPa presents porous structure with well-developed crystals. SEM shows a less dense and open microstructure with large pores due to coupled effect of temperature and pressure. The development of crystals resulting from the transformation of C-S-H to $C_6S_2H_3$ (jaffeite) via α - C_2SH is the main cause of pore structure degradation and compressive strength depletion, as it is presented in Table 2.

Hydrothermal curing of the hardened G-Oil well cement for 7 days provided a decrease in compressive strength compared to cement paste cured under standard condition. The main cause of this strength depletion is the change in pore structure due to the transformation of initial C-S-H to $C_6S_2H_3$ through α - C_2SH crystals.

Engineering properties of cement composites for oil well applications such as strength, permeability, and diffusivity (and thus durability) and shrinkage are intimately

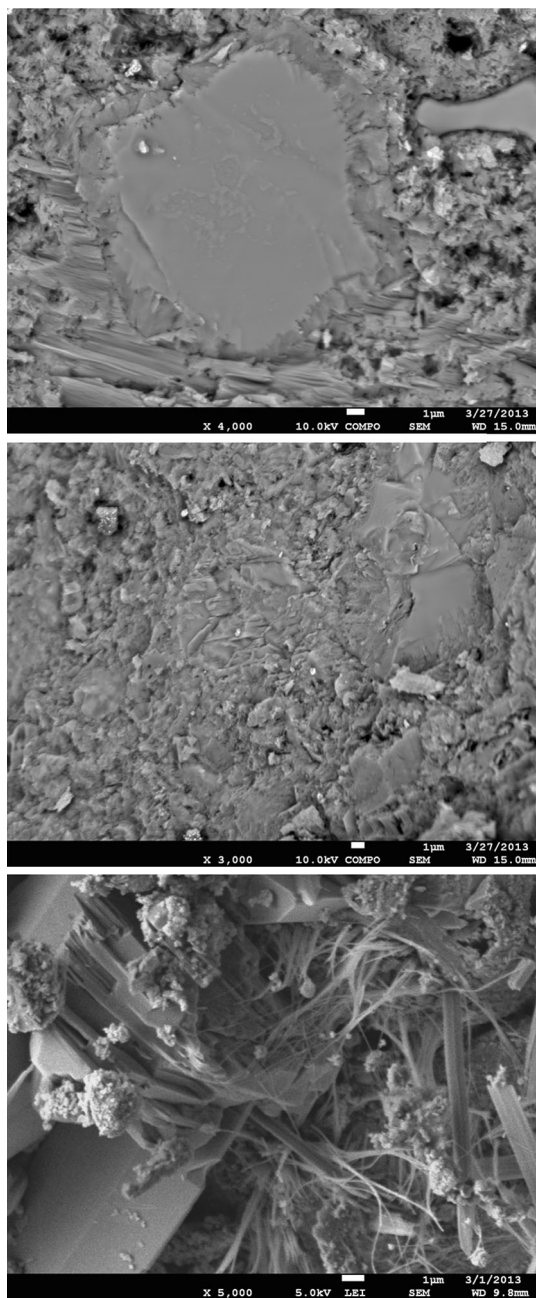


Fig. 7 SEM micrographs of G-Oil well cement cured under standard condition and hydrothermal curing (G0, G0.3, and G1.2)

Table 2 Compressive strength and permeability of cured samples

| | Curing conditions | | |
|-----------------------------------|---|------------------------------------|------------------------------------|
| | Standard 20 °C, 100 % rel. humidity | Hydrothermal 0.3 MPa; 150 °C | Hydrothermal 1.2 MPa; 200 °C |
| Compressive strength/MPa | 77.5 ± 2.0 | 51.8 ± 2.0 | 20.5 ± 1.0 |
| Permeability/ ms ⁻¹ | 2 × 10 ⁻¹⁵ | 7 × 10 ⁻¹⁵ | 199 × 10 ⁻¹⁵ |

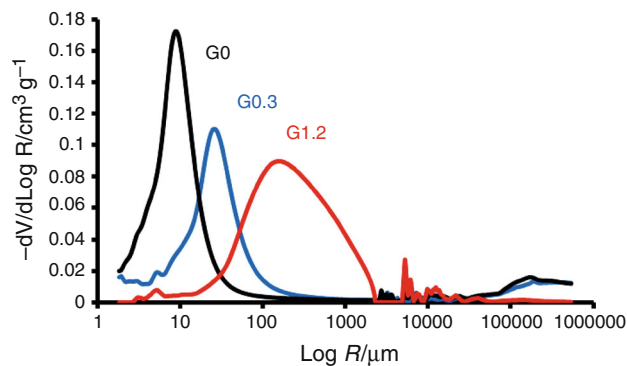


Fig. 8 Influence of curing conditions on the PSD of G-Oil well cement paste

associated with porosity and pore size distribution [21]. The volume and size distribution of pores affect not only the mechanical strength of cement based materials, but also its durability.

The pore size distribution (PSD) of cement pastes cured under different hydrothermal regimes is depicted in Fig. 8. The effect of hydrothermal effect is evidenced by the intensity and position of the peak, by the length and bimodal characteristic of PSD. Permeability coefficient K is one of the essential properties used in evaluation of cement paste durability. It was calculated by software Poremaster during porosimetric analysis according the following model:

$$K = \frac{\phi d_p^2}{32}, \quad (2)$$

where ϕ is the powder bed porosity and d_p the average pore diameter.

This parameter is characteristic for cementitious materials for application in oil well. As it can be seen in Table 2, the permeability coefficient has markedly increased with increasing temperature/pressure. The PSD of samples cured under different conditions is recorded in Fig. 8. With increasing temperature/pressure, curves of PSD are displaced toward higher pore size. This is the demonstration of hydrothermal curing on the pore structure of G-Oil well cement paste.

Conclusions

Cement paste of oil well cement cured under hydrothermal conditions has presented different characteristics at TG and DTG curves. The method has qualitatively and quantitatively identified different hydrated products varying with hydrothermal curing conditions. The main hydration products of cured G-Oil well cement under standard condition are C-S-H gel, Ca(OH)₂, and calcite resulting from the

carbonation of the two first products. With increasing temperature/pressure of hydrothermal curing, peak characterizing the presence of C–S–H decreases as a result of its crystallization into $C_6S_2H_3$ via α - C_2SH . This crystallization causes a reduction in solid volume and is accompanied by an increase in porosity and permeability of cured samples. The transformation of C–S–H to α - C_2SH and $C_6S_2H_3$ under autoclave curing causes the depletion of microstructure and the reduction in compressive strength known as strength retrogression.

Acknowledgements This article has been produced with the financial assistance of the European Regional Development Fund (ERDF) under the Operational Programme Research and Development/Measure 4.2 and with financial support from VEGA No. 1/0064/12. This work was also supported by Project Centers for materials research at FCH BUT, Reg. No. CZ.1.05/2.1.00/01.0012.

References

1. Ježo Ľ, Ifka T, Cvopa B, Škundová J, Kovár V, Palou MT. Effect of temperature upon the strength development rate and upon the hydration kinetics of cements. *Ceram Silik*. 2010;54(3):269–76.
2. Feng L, Christian M. Hydration kinetics modeling of Portland cement considering the effects of curing temperature and applied pressure. *Cem Concr Res*. 2009;39:255–65.
3. Elkhadiri I, Palacios M, Puertas F. Effect of curing temperature on cement hydration. *Ceram Silik*. 2009;53(2):65–75.
4. Zhang J, Weissinger EA, Peethamparan S, Scherer GW. Early hydration and setting of oil well. *Cem Concr Res*. 2010;40:1023–33.
5. Jupe AC, Wilkinson AP, Luke K, Funkhouser GP. Class H cement hydration at 180 °C and high pressure in the presence of added silica. *Cem Concr Res*. 2008;38:660–6.
6. Richardson IG. The nature of C-S-H in hardened cements. *Cem Concr Res*. 1999;29:1131–47.
7. Le Saout G, Lécolier E, Rivereau A, Zanni H. Chemical structure of cement aged at normal and elevated temperatures and pressures part I. Class G oil well cement. *Cem Concr Res*. 2006;36:71–8.
8. Shaw S, Henderson CMB, Clark SM. Hydrothermal formation of hydrated calcium silicates: an in situ synchrotron study. *Am Mineral*. 1998;62A:1337–78.
9. Palou MT, Bágel Ľ. Preparation and properties of cementitious composites for geothermal applications. *Chem Pap*. 2012;66(9):881–90.
10. Kalousek GL. Development of cement for geothermal wells. Final report, work performed for the division of geothermal energy US. Department of Energy Washington, DC 1979.
11. Palou MT, Bágel Ľ, Živica V, Kuliffayová M, Kozánková J. Influence of hydrothermal curing regimes on the hydration of fiber-reinforced cement composites. *J Therm Anal Calorim*. 2013;113:385–94. doi:10.1007/s10973-013-2943-4.
12. Palou MT, Bágel Ľ, Živica V, Kuliffayová M, Ifka T. Hydration of high alumina cement–silica fume composite with addition of Portland cement or sodium polyphosphate under hydrothermal treatment. *J Therm Anal Calorim* 2013;113:385–94. doi:10.1007/s10973-013-3042-2.
13. Smith RC. The use of sea water in well cementing. *J Petrol Technol*. 1975;27:759–64. doi:10.2118/5030-PA.
14. William CL, Gary JP. Standard handbook of petroleum and natural gas engineering. 2nd ed. Oxford: Linacre House, Jordan Hill; 2005.
15. Ramachandran VS, Paroli RM, Beaudoin JJ, Delgado AH. Thermal analysis of construction materials. In: Ramachandra VS, et al., editors. Handbook of thermal analysis of construction materials. New York: Elsevier; 2002. p. 118.
16. Alunno VR, Chioocchio G, Collepardi M. Influence of procuring on high pressure steam hydration of tricalcium silicate. *Cem Concr Res*. 1973;3:665–76.
17. Midgley HG, Chopra SK. Hydrothermal reactions between lime and aggregate fines. *Mag Concr Res*. 1960;12:73–82.
18. Collepardi M, Marches B. Morphology and surface properties of hydrated tricalcium silicate pastes. *Cem Concr Res*. 1972;2:57–65.
19. Drábik M, Gálíková L', Balkovic S, Slade RCT. Potential of Portland cements for MDF materials. *J Phys Chem Solids*. 2003;68:1057–61.
20. Janotka I, Krajčí Ľ, Rayb A, Mojumdar SC. The hydration phase and pore structure formation in the blends of sulfoaluminate–belite cement with Portland cement. *Cem Concr Res*. 2003;33:489–97.
21. Day RL, Marsh BK. Measurement of porosity in blended cement pastes. *Cem Concr Res*. 1988;18:63–73.